Bounding box extraction from spherical hologram of elementary object to synthesize hologram of arbitrary three-dimensional scene with occlusion consideration

(Invited Paper)

Jae-Hyeung Park* **and Hong-Gi Lim**

School of Information and Communication Engineering, Inha University, Inha-ro 100, Nam-gu, Incheon, 402-751, Korea

**Corresponding author: jh.park@inha.ac.kr*

Received March 28, 2014; accepted April 23, 2014; posted online May 28, 2014

A novel method to extract a bounding box that contains the three-dimensional object from its spherical hologram is proposed. The proposed method uses the windowed Fourier transform to obtain the angular distribution of the quasi-collimated beams at each position in the spherical hologram and estimates the bounding box by accumulating the quasi-collimated beams in the volume inside the spherical hologram. The estimated bounding box is then used to realize occlusion effect between the objects in the synthesis of the three-dimensional scene hologram.

OCIS codes: 090.1760, 090.1995, 070.7345.
doi: 10.3788/COL201412.060019.

Holography is a versatile tool in capturing and reproducing the three-dimensional (3D) information of the object[1−3]. Especially, a spherical hologram which contains the optical field on the surface of a sphere surrounding the object has all-around information, making it useful in applications where full 3D information of the object is required. The curved surface of the spherical hologram also makes it more efficient than a planar hologram in terms of the required sampling rate for a given angular spectrum range of the object[4]. Recently, a few studies have been reported to optically record or computationally synthesize and process the spherical hologram of the objects[4−8].

One of the interesting applications of the spherical hologram is the hologram synthesis of a 3D scene from the spherical holograms of elementary objects[8] as illustrated in Fig. 1. In this application, the spherical hologram of the individual elementary 3D object is pre-calculated or optically recorded. These spherical holograms are then used to synthesize a new hologram of a 3D scene that consists of the individual elementary 3D objects. The all-around information contained in the spherical hologram allows the elementary 3D objects to be located at arbitrary positions and with arbitrary orientations in the 3D scene. In this hologram synthesis of the 3D scene, the occlusion between the elementary 3D objects should be considered for more realistic representation of the scene. The occlusion consideration, however, is not trivial since what is available is not the 3D model of the elementary object but only its spherical hologram.

In this letter, we propose a method to extract a bounding box of the 3D object from its spherical hologram. The bounding box is the volume which contains the 3D object. The bounding boxes extracted from the spherical holograms are used to consider occlusion between the elementary objects in the hologram synthesis of the 3D scene.

One simple way to extract the bounding box is to consider the sampling interval of the spherical hologram. The maximum local spatial frequency along the azimuthal $f_{l\varphi}$ and polar angle direction $f_{l\theta}$ of the spherical hologram is given by[4],

$$|f_{l\varphi}|_{\max} = |f_{l\theta}|_{\max} = \frac{r_{\mathrm{o,\,max}}}{\lambda}, \tag{1}$$

where λ is the wavelength and $r_{\mathrm{o,\,max}}$ is the maximum radial distance of the object point from the origin of the spherical hologram. From the Nyquist criterion, the sampling interval $\Delta\varphi$ and $\Delta\theta$ of the spherical hologram should satisfy $\Delta\varphi < 1/2|f_{l\varphi}|_{\max}$, $\Delta\theta < 1/2|f_{l\theta}|_{\max}$. Thus the bounding box can be defined as spherical volume as shown in Fig. 1 with radius r_{b} given by

$$r_{\mathrm{b}} = \min\left[\frac{\lambda}{2\Delta\varphi},\ \frac{\lambda}{2\Delta\theta}\right] \geqslant r_{\mathrm{o,\,max}}, \tag{2}$$

where min [•] is the function that returns smaller value among the argument, and it is used here for the case of over-sampling. This method is simple and effective in finding the maximum spherical volume wherein the object is contained without aliasing in the spherical hologram surface. However, this spherical bounding box does not reflect actual shape and size of the object, and thus it tends to over-occlude rear elementary objects in the 3D scene hologram synthesis.

The method we propose in this Letter extracts more refined bounding box based on Windowed Fourier transform (WF) of the spherical hologram. Figure 2 illustrates the proposed method. Each spatial frequency component of an optical field corresponds to a plane wave of a specific propagation direction. The WF of the hologram gives spatial frequency spectrum at the local hologram patch position where the calculation window is located, and thus gives angular distribution of the quasi-collimated

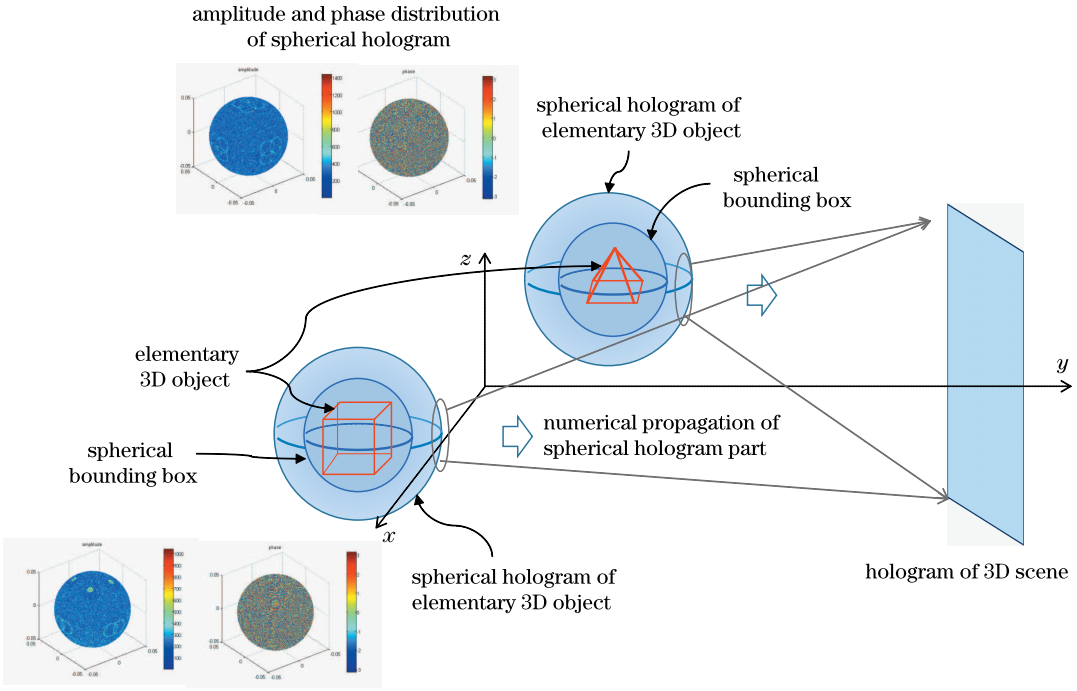

Fig. 1. Synthesis of 3D scene hologram from spherical holograms of elementary objects.

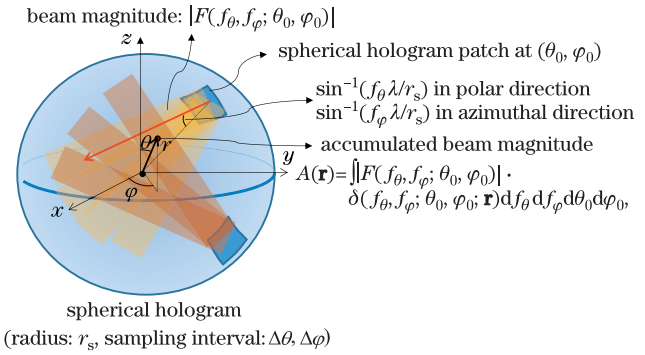

Fig. 2. Proposed method to extract the refined bounding box from the spherical hologram.

beams from the hologram patch. By accumulating these quasi-collimated beams in the volume inside the spherical hologram, the region where the 3D object is located can be identified.

More specifically, suppose a spherical hologram with the number of sampling points $N_\varphi = 2\pi/\Delta\varphi$ and $N_\theta = \pi/\Delta\theta$ in azimuthal and polar direction, respectively. The WF F of the spherical hologram U with the calculation window of the size $L_\varphi \times L_\theta$ centered at (θ_o, φ_o) is given by

$$F(f_\theta,\ f_\varphi;\ \theta_o,\ \varphi_o) = \iint U(\theta,\ \varphi)\, W\left(\frac{\theta-\theta_o}{L_\theta},\ \frac{\varphi-\varphi_o}{L_\varphi}\right) \cdot \exp\left[-j2\pi\left(f_\theta\theta + f_\varphi\varphi\right)\right] \mathrm{d}\theta\mathrm{d}\varphi, \quad (3)$$

where W is the window function satisfying $W(\theta, \varphi)=1$ for $|\theta, \varphi| < 1/2$, and $W(\theta,\varphi)=0$ otherwise. In the proposed method, the absolute value $|\mathrm{F}(f_\theta, f_\varphi; \theta_o, \varphi_o)|$ is used as the magnitude of the quasi-collimated beam of the width $r_s L_\varphi \sin\theta \times r_s L_\theta$, where r_s is the radius of the spherical hologram. The propagation direction of the beam has the angle $(\sin^{-1}(f_\theta\lambda/r_s), \sin^{-1}(f_\varphi\lambda/r_s))$ in polar and azimuthal direction with respect to the inward normal of the spherical hologram patch at (θ_o, φ_o). These quasi-collimated beams are accumulated inside the spherical hologram, giving

$$A(\mathbf{r}) = \int |F(f_\theta, f_\varphi; \theta_o, \varphi_o)|\, \delta(f_\theta, f_\varphi, \theta_o, \varphi_o; \mathbf{r}) \mathrm{d}f_\theta \mathrm{d}f_\varphi \mathrm{d}\theta_o \mathrm{d}\varphi_o, \quad (4)$$

where $\delta(f_\theta,\ f_\varphi;\ \theta_o,\ \varphi_o;\ \mathbf{r})$ is a delta function which is nonzero only when the quasi-collimated beam defined by $(f_\theta,\ f_\varphi;\ \theta_o,\ \varphi_o)$ passes through the position defined by the position vector $\mathbf{r}$. Since the quasi-collimated beams converge at the object points, the accumulated beam magnitude $\mathrm{A}(\mathbf{r})$ has larger value where the elementary 3D object is located and thus $\mathrm{A}(\mathbf{r})$ represents the shape and region of the object.

In the proposed method, the synthesis of the 3D scene hologram from the elementary spherical holograms with occlusion consideration is performed using $\mathrm{A}(\mathbf{r})$ as illustrated in Fig. 3. For each position P in the 3D scene hologram, the corresponding part B in each spherical hologram is found by projecting the spherical bounding box given by Eq. (2) onto the spherical hologram with P as a projection vanishing point. Note that this spherical hologram part B is the maximum area that can contribute to the 3D scene hologram point without aliasing. For each spherical hologram point S in this part, the complex magnitude is scaled by

$$\widetilde{U}_\mathrm{m}(S) = U_\mathrm{m}(S)\left\{c_\mathrm{g}\int_{S'S} A_\mathrm{m}(\mathbf{r})\mathrm{d}l\right\} \cdot \left\{1 - c_\mathrm{a}\sum_n \int_{\mathrm{SP}} A_n(\mathbf{r})\mathrm{d}l\right\}, \quad (5)$$

where $U_\mathrm{m}(S)$ is the original complex magnitude at position S of the m-th spherical hologram, S′ is the intersec-

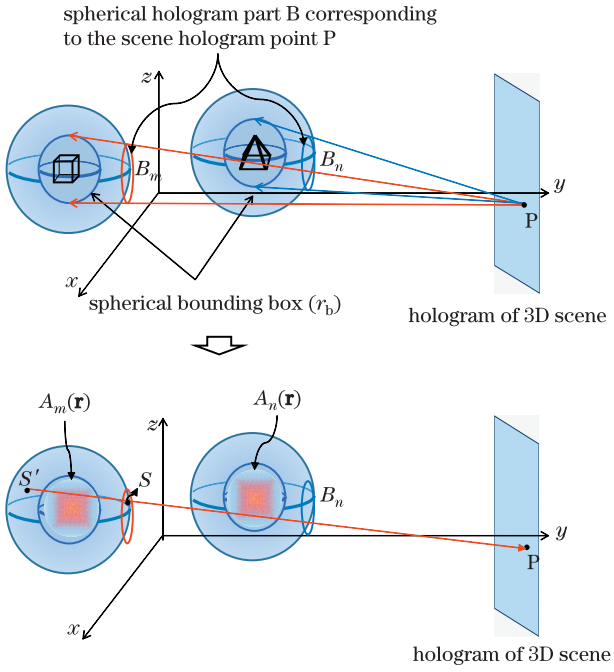

Fig. 3. Occlusion consideration in the 3D scene hologram synthesis using proposed method.

tion of the extension of the line SP with the m-th spherical hologram, $A_{\mathrm{m}}(\mathbf{r})$ and $A_n(\mathbf{r})$ are the accumulated beam magnitude of the m-th and n-th spherical hologram and c_{g} and c_{a} are the coefficients that control the gain and the attenuation. In Eq. (5), the first part multiplied to $U_{\mathrm{m}}(S)$ represents the possibility that the line S′S actually meets the m-th object, and thus acts as the gain factor of the complex magnitude. The summation in the second part represents the possibility that the line SP is occluded by other objects and thus the second part acts as the attenuation factor. Therefore the complex amplitude scaling given by Eq. (5) reduces the contribution of the spherical hologram points which do not lie in the line from the corresponding object to the hologram point or are occluded by the other objects, realizing the occlusion effect. The hologram synthesis of the 3D scene is finally performed using the scaled complex magnitude by

$$H(P)=\sum_i \iint_{B_i} \widetilde{U}_i(S)\frac{\exp(jkr_{\mathrm{SP}})}{r_{\mathrm{SP}}}\mathrm{d}s, \quad \text{for} \quad S\in B_i, \quad (6)$$

where k is the wave number and the r_{SP} is the distance between two points S and P.

We verified the proposed method using computer generated spherical holograms. The elementary 3D objects used in the verification are a pyramid of 7×7×7 (mm) size and a squeezed hexahedron of 4×14×14 (mm) size. Spherical holograms were synthesized for two objects with radius 50 mm and sampling interval $\Delta\theta$=$\Delta\varphi$=0.0027 rad, giving 1181(θ)×2362(φ) resolution for each. The spherical holograms were located such that their centers coincide with the centers of the corresponding objects. The wavelength was assumed to be 100×532 nm where 100× scaling was used to reduce the required hologram resolution and thus reduce the calculation time and memory requirement in the verification.

Figure 4 shows the phase of the calculated spherical holograms. Note that from Eq. (2) the bounding box radius r_{b} is given by r_{b}=10 mm for both holograms, and thus the pyramid object is well inside the spherical bounding box. The maximum radial distance of the squeezed hexahedron object is 10.1 mm which is slightly larger than r_{b}. The difference, however, is not large and thus the aliasing was not considered in the following verification. For these spherical holograms, the accumulated beam magnitude A($\mathbf{r}$) was calculated using WF by Eq. (4). The number of samples ($L_\varphi/\Delta\varphi$, $L_\theta/\Delta\theta$) of each spherical hologram patch used in the WF is 40(θ)×40(φ). Figure 5 shows the contour slices of the calculated and normalized A($\mathbf{r}$) with the original object indicated by black dots. It can be seen that the region where A($\mathbf{r}$) has larger value is well matched to the actual object, proving the A($\mathbf{r}$) of the proposed method estimates the shape and the region of the object from its spherical hologram successfully.

Using the calculated A($\mathbf{r}$), the 3D scene hologram was synthesized. Two spherical holograms, the pyramid and the squeezed hexahedron, were rotated by $\pi/4$ rad (θ) and $\pi/6$ rad (φ), and located at (−3 mm, 10 mm, 0 mm), and (3 mm, −10 mm, −3 mm), respectively. The planar hologram of the 3D scene was located at y=300 mm plane and has 200×200 resolution with 0.25-mm sampling interval. For each planar hologram point P, the corresponding spherical hologram parts $\mathrm{B}_{\mathrm{pyramid}}$ and $\mathrm{B}_{\mathrm{hexahedron}}$ were found by projection of the spherical bounding box. In the verification, $\mathrm{B}_{\mathrm{pyramid}}$ and $\mathrm{B}_{\mathrm{hexahedron}}$ were the circular portions of the spherical holograms containing 12525 and 12647 sampling points in the spherical holograms, respectively. Figure 6 shows the synthesized 3D hologram and Fig. 7 shows its numerical reconstructions of 200×200 resolution. In Fig. 7, it can be observed that the rear hexahedron object is

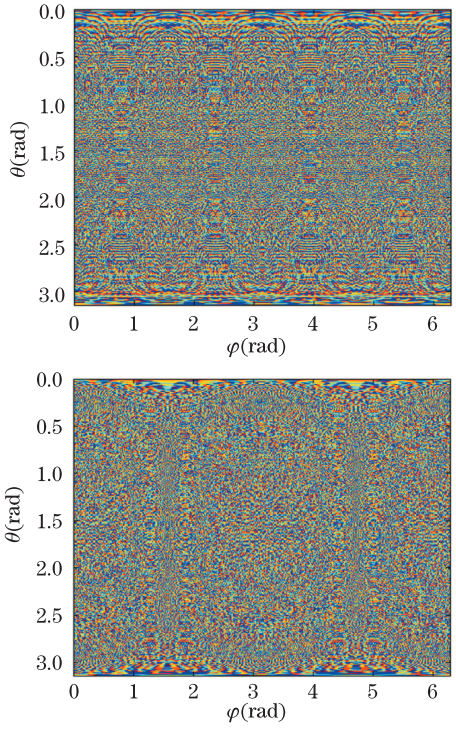

Fig. 4. Spherical holograms for (a) pyramid object and (b) squeezed hexahedron object.

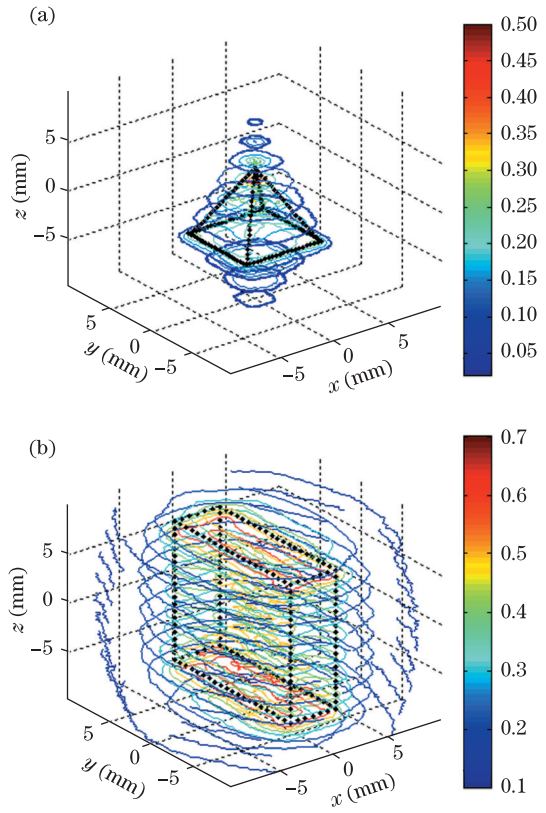

Fig. 5. Contour slices of the accumulated beam magnitude using proposed method with original object indicated in black dots; (a) pyramid object, (b) squeezed hexahedron object.

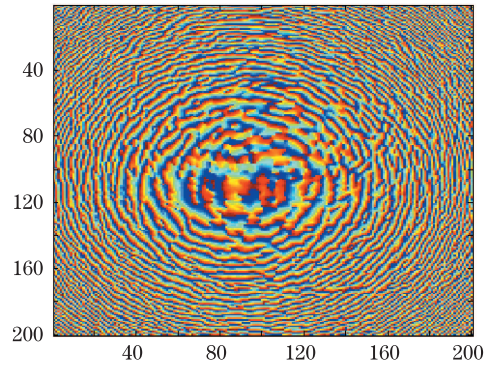

Fig. 6. Synthesized planar hologram of the 3D scene.

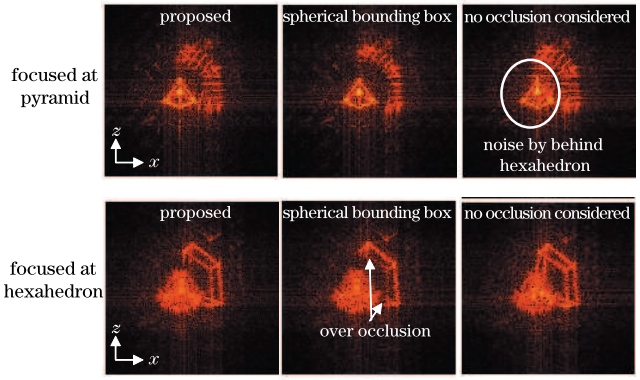

Fig. 7. Numerical reconstruction of the 3D scene hologram.

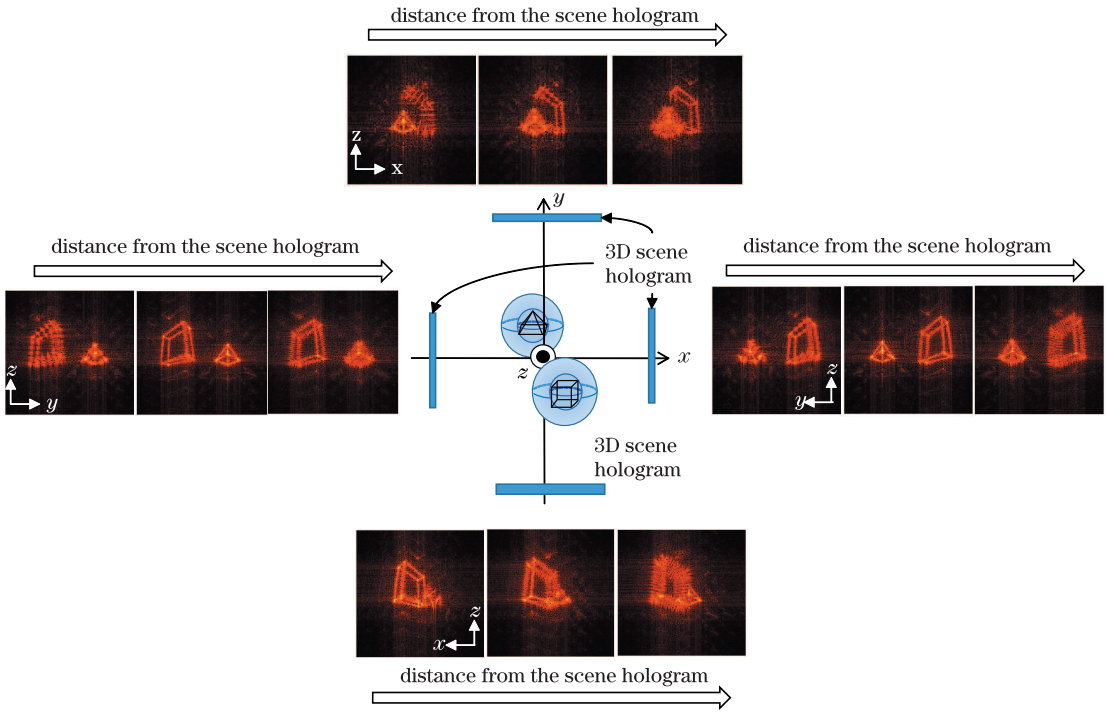

Fig. 8. Numerical reconstruction of the 3D scene holograms at four different positions.

occluded by the front pyramid object successfully in the proposed method. On the contrary, when only spherical bounding box given by Eq. (2) is considered, the rear hexahedron object is over-occluded losing lines as shown in Fig. 7. Figure 7 also shows that the reconstruction of the front pyramid object is ruined when occlusion is not considered. Therefore, from the results shown in Figs. 5 and 7, it is verified that the proposed method can

estimate the object shape and region from its spherical hologram and it can be used to realize the occlusion effect in the synthesis of the 3D scene. Figure 8 is another result where the scene hologram is located at 4 different positions. The numerical reconstructions show that the objects are reconstructed at their relative positions with proper occlusions successfully.

In this letter, a novel method to extract the object shape and region from its spherical hologram using WF is proposed. The proposed method accumulates the magnitudes of the quasi-collimated beams from every part of the spherical hologram. The beam magnitude accumulated in the volume inside the spherical hologram represents the object shape and region, and this accumulated beam magnitude is used to realize the occlusion in the 3D scene hologram synthesis from the spherical holograms of elementary objects. The verification performed using computationally generated holograms confirms the feasibility of the proposed method successfully.

This work was partly supported by 'The Cross-Ministry Giga KOREA Project' of The Ministry of Science, ICT and Future Planning, Korea. [No. GK13D0100, Development of Telecommunications Terminal with Digital Holographic Table-top Display]. This work was also partly supported by the Basic Science Research Program through the National Research Foundation of Korea (NRF) funded by the Ministry of Education (No. 2013-061913).

References

1. B. Lee, Phys. Today **66,** 36 (2013).
2. J. Hong, Y. Kim, H.-J. Choi, J. Hahn, J.-H. Park, H. Kim, S.-W. Min, N. Chen, and B. Lee, Appl. Opt. **50,** H87 (2011).
3. S.-G. Park, J. Yeom, Y. Jeong, N. Chen, J-Y. Hong, and B. Lee, J. Inf. Disp. **15,** 37 (2014).
4. G. Li. A.-H. Phan, N. Kim, and J.-H. Park, Appl. Opt. **52,** 3567 (2013).
5. O. D. D. Soares and J. C. A. Fernandes, Appl. Opt. **21,** 3194 (1982).
6. M. L. Tachiki, Y. Sando, M. Itoh, and T. Yatagai, Appl. Opt. **45,** 3527 (2006).
7. B. J. Jackin and T. Yatagai, Opt. Express **21,** 935 (2013).
8. K. Hosoyachi, K. Yamaguchi, T. Ichikawa, and Y. Sakamoto, Appl. Opt. **52,** A33 (2013).